Food Research International 161 (2022) 111855

Contents lists available at ScienceDirect

Food Research International

journal homepage: www.elsevier.com/locate/foodres

Chitosan suspension as extractor and encapsulating agent of phenolics from acerola by-product

Natalia Cristina da Silva [a,b], Odílio Benedito Garrido Assis [b], Alan Giovanini de Oliveira Sartori [c], Severino Matias de Alencar [c], Milena Martelli-Tosi [a,d,*]

[a] Department of Food Engineering, Faculty of Animal Science and Food Engineering, University of São Paulo, Rua Duque de Caxias Norte 225, CEP 13635-900, Pirassununga, SP, Brazil
[b] National Nanotechnology Laboratory for Agriculture, Embrapa Instrumentação, Rua XV de Novembro, 1452, CEP 13561-206, São Carlos, SP, Brazil
[c] Department of Agri-food Industry, Food and Nutrition, Luiz de Queiroz College of Agriculture, University of São Paulo, Av. Pádua Dias, 11, CEP 13418-900, Piracicaba, SP, Brazil
[d] Departament of Chemistry, Faculty of Philosophy, Sciences and Letters of Ribeirão Preto, University of São Paulo, Av. Bandeirantes, 3900, CEP 14040-901, Ribeirão Preto, SP, Brazil

ARTICLE INFO

Keywords:
Food residue
Active compounds
Nanoencapsulation
Drug carrier

ABSTRACT

The polymeric suspension of chitosan (Ch) has been an effective media for the extraction of total phenolic compounds (TPC) from the acerola by-product. It facilitates the subsequent production of nanoparticles loaded with the phenolics (Np-TPC) by ionic gelation. However, neither the effects of Ch concentration on encapsulation efficiency (EE%) of TPC nor which compounds are extracted in its media are known, being it the first objective of this study. The second objective was to analyze the stability of the Np-TPC under accelerated conditions and its release profile at pHs 3.0 and 7.0. The results showed that Ch does not affect the extraction of TPC. However, the EE increased from 35.0 to 48.1 % with the increase of Ch concentration (0.4 to 1.0 %). LC/ESI-QTOF MS analysis showed that phenolic acids and flavonoids are extracted in 0.8 % Ch medium. After encapsulation, microscopy images revealed particle sizes ranging between 110 and 150 nm. Additionally, the presence of phenolics did not change the stability of the particles under accelerated conditions and the actives were fully released into the released medium for 10 h. The Np-TPC suspension appears to be useful for the production of edible antioxidant coatings to preserve fruits/vegetables, with potential application as carrier of other food ingredients.

1. Introduction

Acerola *(Malpighia* spp.*)* is a tropical fruit of added economic value with a significant share in the export market of Brazil, the world's largest producer. The estimated average productivity in the country is about 150 thousand tons of fruit per year, of which 54 % is directed to the fresh fruit consumption market and 46 % to industrial processing. This processing is an economic alternative for the use of the fruit, but it results in up to 41 % of by-products (peels and seeds) (Mendes et al., 2012; Abreu et al., 2020). Most of these by-products contain important levels of active and antioxidants compounds, such as phenolic compounds, which are commonly found in by-products from ripe fruit (Silva, Barros-Alexandrino, Assis & Martelli-Tosi 2021; Poletto et al., 2021).

In recent studies conducted by Paletto et al. (2021) and Gualberto et al. (2021), using Liquid Chromatography Coupled to Mass Spectrometry (LC-MS/MS), some of the main phenolic compounds identified in the acerola by-product were: catechin, epicatechin, caffeic acid, 2-hydroxycinnamic acid, ferulic acid, rutin, quercetrin, quercetin, kaempferol and (iso)formononetin. All of them are mainly known for their antioxidant activities in addition to other important health features such as anti-inflammatory effect (Ko et al., 2020); improvement of enzymatic activity, mitochondrial functionality (Alvarez-Suarez et al., 2017); broad antimicrobial properties (Lima et al., 2021).

Phenolic compounds can be used as food bioactives in a wide range of applications like edible coatings to preserve fruits (Silva et al., 2021) or even additives (Skendi et al., 2022). However, they can be chemically or physically unstable depending on environmental conditions, such as oxygen, pH, light, enzymatic degradation and temperature. Micro/

* Corresponding author at: Laboratory of Encapsulation and Functional Foods (LENALIS), Department of Food Engineering – University of São Paulo, Av. Duque de Caxias Norte, 225, 13635-900 Pirassununga, São Paulo, Brazil.
E-mail address: mmartelli@usp.br (M. Martelli-Tosi).

https://doi.org/10.1016/j.foodres.2022.111855
Received 30 May 2022; Received in revised form 12 August 2022; Accepted 21 August 2022
Available online 25 August 2022

nanoencapsulation is one of the alternatives which have been widely studied in order to overcome these drawbacks (Akcicek, Bozkurt, Akgül & Karasu, 2021, Esposto et al., 2021, Javadian, Shahosseini & Ariaii, 2017, Maleki, Woltering & Mozafari, 2022). Chitosan and chitosan-based nanoparticles are being successfully considered for delivering of food bioactives due to their biodegradability and biocompatibility (Esposto et al., 2021, Maleki et al., 2022).

In the traditional methodology of chitosan nanoparticle formation, the actives are either added directly in the chitosan solution or they are first extracted in a solvent, concentrated and then incorporated into chitosan solution, prior to cross-linking by ionic gelation (Britto et al., 2014, Esposto et al., 2022). The solvent used in the extraction of active compounds is an important point to be considered. Typically, organic solvents (ethanol, methanol or acetone) are used, ensuring that high amounts of compounds are obtained (Gualberto et al., 2021; Silva et al., 2021). Despite the good extraction efficiency, these solvents can generate liquid waste that is harmful to humans and the environment. To minimize this problem, a new methodology has been proposed in which phenolic compounds are extracted directly in a mild acidic chitosan solution (Silva et al., 2021; Silva & Martelli-Tosi, 2021). Direct extraction into the medium eliminates solvent evaporation and the resulting suspension is suitable for nanoparticle processing by ionic gelation. Moreover, the enriched chitosan suspension can be readily transformed into edible films or coatings. This procedure can be considered as a sustainable alternative from a waste generation point of view.

Although the method of direct use of chitosan as an extractor of actives from acerola by-product has shown similar efficiencies to organic solvents (Silva et al., 2021; Silva & Martelli-Tosi, 2021), some points still require understanding: i) What is the influence of the chitosan concentration on the effectiveness of extracting the actives and their subsequent encapsulation? ii) Which phenolics are extracted and encapsulated? iii) What is the stability of the formed nanoparticles under accelerated conditions and different pH media?

2. Material and methods

2.1. Material

Acerola pulp by-products (peels and seeds) were supplied by Dal Bon Polpas (São José do Rio Pardo, SP, Brazil). The acerola by-products were dried at 40 °C for 48 h and milled using a knife mill (Marconi, Piracicaba, SP, Brazil).

Chitosan of medium molecular weight (Product 448877, MW ranging from 190,000 to 310,000 g/mol, with 75–85 % deacetylated units), sodium tripolyphosphate (MW of 367.86 g/mol), acetic acid, gallic acid, quercetin, 2,2′-azino-bis(3-ethylbenzothiazoline-6-sulfonic acid) (ABTS), and Folin-Ciocalteu reagent were purchased from Sigma Aldrich (Missouri, USA). Aluminum chloride ($AlCl_3$), potassium chloride (KCl), sodium acetate ($C_2H_3NaO_2$), sodium carbonate (Na_2CO_3), and oxalic acid ($C_2H_2O_4$) were purchased from Labsynth (Diadema, SP, Brazil). Ascorbic acid ($C_6H_8O_6$) was obtained from LS Chemicals (Ribeirão Preto, SP, Brazil). Ultrapure deionized water was prepared using a Direct-Q3 Ultrapure Water System from Millipore (Bedford, MA, USA), with a resistance of 18.2 MΩ.cm.

2.2. Acerola by-product characterization

2.2.1. Centesimal composition

The by-product was characterized according to: moisture (AOAC 925.45), mineral matter (AOAC 926.12), crude fiber (AOAC 985.29), ether extract (AOAC 920.39C), and crude protein (AOAC 923.05/AOAC 991.29) (AOAC, 1997). Total carbohydrates were calculated by difference.

2.2.2. Exhaustive extraction to determine active compounds and antioxidant activities

The exhaustive extraction methodology (Rodrigues, Mariutti & Mercadante, 2013) was used to estimate the active compounds and antioxidant activities of the by-product. To extract the active portion, by-product (1 g) was mixed with 10 mL of methanol:water (8:2, v:v) under agitation on an orbital shaker (Marconi, Piracicaba, SP, Brazil) for 30 min, followed by centrifugation (8000 rpm, 10 °C, 10 min) (Hettich, Universal 320, Brazil). The remaining solid residue was re-extracted with fresh solvent. The process was repeated until the compounds were no longer identified in the solution. The values collected in each supernatant were summed up to determine the total amount of compounds.

The total phenolic compounds (TPC) content was estimated by the Folin-Ciocalteu colorimetric method (Swain & Hillis, 1959). The TPC was calculated using the analytical curve for equivalent gallic acid (GAE) and expressed in mg GAE/100 g by-product on a dry basis (d.b).

The total flavonoids content was determined according to Funari & Ferro (2006). The quantification was performed using the analytical curve for quercetin and the flavonoid's content was expressed in mg quercetin/100 g by-product (d.b).

The anthocyanins content was determined according to Lee, Durst & Wrolstad (2005). The quantification was carried out using the Eq. (1), where A is the difference in absorbance values measured at each wavelength for both pH; ε is the molar coefficient of cyanidin-3-glycoside (26900 L/cm); L is the cuvette width; FD is the sample dilution factor, and PM is the molecular weight of cyanidin-3-glycoside (449.2 g/mol). The anthocyanin's content (CA) was expressed in mg cyanidin-3-glycoside/100 g by-product (d.b).

$$CA = \left[\frac{A}{ExL}\right] \times 1000 \times FDxPM \quad (1)$$

The antioxidant capacity of each supernatant was analyzed by ABTS free radical (Re et al., 1999) and Ferric Reducing Antioxidant Power (FRAP) (Pulido, Bravo, & Saura-Calixto, 2000) methods. For the quantification, an analytical curve for equivalent Trolox (ET) was used and the antioxidant capacity expressed in μMol ET/100 g by-product (d.b).

2.2.3. Determination of vitamin C content

Vitamin C extraction was carried out in 2 % oxalic acid (v:v). The mixture was stirred on an orbital shaker at room temperature for 2 h and the supernatant was analyzed by liquid chromatography (Shimadzu, Japan). Chromatographic conditions were based on Baierle et al. (2012), with modifications. Separation was performed on a C18 Shim-pack GIST reversed phase column (250 mm × 4.6 mm, 5 μm) at 30 °C. Ultrapure water with pH 3.0 was used as the mobile phase. The analyis was carried under isocratic mode at a flow rate of 1 mL/min with a run time of 10 min and detection at 245 nm using a diode array detector. Vitamin C peak was identified by comparing their retention time with those of standard ascorbic acid.

2.3. Extraction and encapsulation of TPC in chitosan suspension

The extraction and encapsulation of TPC were performed according to the methodology described by Silva et al. (2021) and Silva & Martelli-Tosi (2021).

4, 6, 8 and 10 mg of chitosan was dissolved in 1 mL of acetic acid (1 %, v:v) using a magnetic stirrer (room temperature, 24 h), resulting in 0.4, 0.6, 0.8 and 1.0 % chitosan suspensions (Ch), respectively. 6 g of dry by-product were added to 100 mL of the 0.4, 0.6, 0.8 or 1.0 % Ch. The by-product:Ch proportion (g:mL) was determined in preliminary tests. The mixtures were submitted to tip ultrasound for TPC extraction (amplitude of 40 %, 550 W, 10 min) (Sonifier SFX550, Branson Ultrasonics, USA), centrifuged (10 °C, 8000 rpm, 15 min) and filtered. The filtrates consisting of chitosan with TPC extract (Ch-TPC) were analyzed

according to TPC content (mg GAE/100 mL Ch-TPC) (Swain & Hillis, 1959). The extraction performed in acetic acid (1 %) was used as a control. All experiments were performed in triplicate.

The four Ch-TPC extracts, produced with 0.4, 0.6, 0.8 and 1.0 % Ch, were encapsulated by the ionic gelation method, by dripping TPP aqueous solution into equal volume of Ch-TPC. The chitosan:TPP ratio was maintained at 3:1 (w:w). The preparation parameters were: flow rate of the TPP of 1 mL/min, circulation intensity of the chitosan suspension of 1500 rpm, and drip height of 8 cm. Finally, nanoparticles loaded with TPC suspensions were obtained (Np-TPC).

2.4. Characterization of nanoparticles

2.4.1. Encapsulation efficiency of TPC

After the production of Np-TPC, the encapsulation efficiency (EE%) of TPC was determined using Amicon Ultra-0.5 Centrifugal Filter Unit 30 KDa membrane (Millipore, Bedford, USA). The Np-TPC suspension was added on the filter and centrifuged (10 °C, 8000 rpm, 15 min) in order to isolate the encapsulated portion from the filtered (non-encapsulated fraction). The EE% was calculated according to Eq. (2), where *Nt* is the content of TPC in total suspension and *Ns* is the content of TPC in the non-encapsulated filtered portion. The results were expressed as % of encapsulated TPC in relation to the total suspension.

$$EE\% = \left[\frac{Nt - Ns}{Nt}\right] \times 100 \quad (2)$$

2.4.2. Size distribution and zeta potential

Np-TPC suspensions were analyzed according to size distribution by Dynamic Light Scaterring (DLS) and zeta potential, using a Zeta Potential Analyzer (Zetasizer ZS 3600, Malvern Instruments, UK), at a detection angle of 173° and wavelength of 633 nm. Samples of chitosan nanoparticles without TPC (Np) were analyzed for control. Measurements were performed in triplicate at 25 °C. After this analysis, samples of Np-TPC and Np with 0.8 % chitosan were used for the other analyzes of the work.

2.4.3. Phytochemical profile of encapsulated compounds by LC/ESI-QTOF MS

The phenolics encapsulated in 0.8 % chitosan nanoparticles were determined by high-performance liquid chromatography coupled with electrospray ionization-quadrupole-time of flight-mass spectrometry (LC/ESI-QTOF MS). Before the encapsulation, Ch-TPC extract was freeze-dried for 48 h, dispersed in 80 % methanol (1:10, m:v), and kept under agitation on an orbital shaker for 2 h. After centrifugation, the supernatant was used for analysis.

Firstly, the sample was submitted to solid phase extraction to remove the sugars, following the procedure described by Soares et al. (2019). Thereafter, liquid chromatography analysis was performed on a Shimadzu chromatograph (Shimadzu Co., Tokyo) equipped with a Phenomenex Luna C18 column (250 × 4.6 × 5 μm) and coupled with a Quadrupole Time-of-Flight (QTOF) mass spectrometer (MAXIS 3G, Bruker Daltonics, Bremen, Germany) with an electrospray ionization (ESI) source operating in the negative mode. The parameters used were reported by Soares et al. (2019). All compounds were tentatively identified by comparison with the standard masses, MS/MS mass spectra, and molecular formulas from available databases and literature. Data analysis was carried out using MAXIS 3G software (Bruker Daltonics, version 4.3).

2.4.4. Field emission scanning electron microscopy

The morphology of Np-TPC and Np was observed under field emission scanning electron microscopy (FEG JSM-5701F, Jeol, USA) by dropping a diluted solution (1:50, v:v) onto a silicon wafer and allowed to dry for 48 h. The samples were coated with platinum.

2.4.5. Attenuated total reflection fourier transform infrared spectroscopy (ATR-FTIR)

To identify the main bands and investigate potential ionic interactions between the groups present in Ch and TPC, in isolated or encapsulated form, FTIR spectra were obtained. A FTIR-ATR Shimadzu spectrophotometer (IR Prestige-21, Shimadzu, Japan) was used. The suspensions were freeze dried for 48 h before analysis. TPP samples were also analyzed. Each spectrum was considered as the average of over 40 individual scans recorded at a resolution of 2 cm^{-1} from 4000 cm^{-1} to 400 cm^{-1}.

2.4.6. Accelerated stability analysis

The physical stability of Np-TPC and Np suspensions, was observed using a multi-sample analytical photocentrifuge (8 mL of sample, time 3600 s, time interval 10 s, at 25 °C) (LUMiSizer, L.U.M. GmbH, Germany). The instability index was calculated as the ratio of the particles that were separated by centrifugal forces.

2.4.7. Release profile

The release profile of TPC from the Np-TPC suspension, was based on the methodologies used by Britto et al. (2014) and Caddeo et al. (2016). The analysis was performed in an incubator at 37 °C under constant agitation (130 rpm). Two different buffered solutions of pH 3 and 7 were used.

The sample was centrifuged and the supernatant (unencapsulated portion) discarded. The pH 3 solution was added over the encapsulated portion and the release evaluated along 2 h. At given times in the intervals, an aliquot of the medium was collected and a new aliquot, at pH 3, was added. The collected aliquot was analyzed concerning the TPC content, and the result expressed as a function of GAE, as previously described. At the end of 2 h, the pH 3 solution was replaced by a pH 7 solution and the experiment continued for 8 h.

2.5. Statistical and graphical analyses

The experimental data means were statistically evaluated and compared by Tukey's test with significance set at $p < 0.05$, using the software Statistica 7.0 (Stat Soft Inc, Tulsa, USA). Mathematical fittings and graphic analyses were performed using Microcal Origin 8.5 software (OriginLab Co, Northampton, MA, USA).

Table 1
Centesimal composition, active compounds contents (vitamin C, flavonoids, anthocyanins and total phenolic compounds (TPC)) and antioxidant activities (ABTS and FRAP) of dry acerola pulp by-product (40 °C, 24 h), expressed on dry basis.

Analysis	Content
Moisture (g/100 g)	7.2 ± 0.2
Mineral matter (g/100 g)	2.0 ± 0.0
Ether extract (g/100 g)	1.0 ± 0.3
Proteins (g/100 g)	8.4 ± 0.0
Fibers (g/100 g)	35.6 ± 0.3
Carbohydrates (g/100 g)	56.7 ± 0.0
Vitamin C (mg/100 g)	Not detected*
Flavonoids (mg quercetin/100 g)	357.8 ± 8.5
Anthocyanins (mg cyanidin-3-glycoside/100 g)	41.4 ± 1.3
TPC (mg GAE/100 g)	1835.4 ± 33.4
ABTS (μMol TE/g)	189.0 ± 2.4
FRAP (μMol TE/g)	201.5 l carbohydrates were calculated by difference.± 0.6

* Fig. A.1.

3. Results and discussion

3.1. Acerola by-product composition

Acerola by-products still have high concentrations of macronutrients and active compounds, as can be observed in Table 1. The macronutrient content obtained in this study is in agreement with data reported in the literature (Monteiro, Barbosa, Silva, Bezerra & Maia, 2020; Silva et al., 2021), with carbohydrates and fiber accounting for > 90 % of the total. Concerning active compounds, phenolics (TPC, quercetin and cyanidin-3-glycoside) were the major class quantified in the by-products. This class of compounds is responsible for the antioxidant capacity of the by-product, confirmed by ABTS and FRAP analyses (Rezende, Nogueira & Narain, 2017; Silva et al., 2021; Shahosseini et al., 2022).

3.2. Effect of chitosan concentration on TPC extraction and encapsulation

Fig. 1 shows the effect of chitosan concentration on TPC extraction and on the efficiency of encapsulation. Chitosan in the concentration range of 0.4–1.0 % did not affect the extraction, since there was no significant difference in the amount of TPC extracted (Fig. 1). When using only acetic acid solution as medium of extraction (Control), the TPC extraction was found to be 15 % (86.99 mg GAE/100 mL extract) higher than the average TPC value extracted by chitosan medium (73.55 mg GAE/100 mL extract). This indicates the polymer concentration has no statistically significant influence on the extraction.

Regarding EE%, Fig. 1 shows that unlike the amount of TPC extracted, the concentration of chitosan has an effect on the TPC encapsulation efficiency. The effect follows a perfectly exponential relationship with the concentration according to a generic function $Y = Ae^x$ with $R^2 = 0.99$. This behavior can be explained by the availability of chitosan active sites. In acidic medium, chitosan is protonated and generates positive charged amino groups (NH_3^+), which are the main interaction sites. So, an increase in chitosan concentration results in more active sites for interaction (Liu & Gao, 2008). In parallel, studies suggest that the hydroxyl (–OH) and carbonyl (-C═O) groups of phenolics have a less positive charge density than chitosan. Therefore, electrostatic interactions (Liang et al., 2017; Bozic, Gorgieva & Kokol, 2012) or hydrogen bonds (Pulicharla, Marques, Das, Rouissi & Brar, 2016) can be occurred between chitosan and phenolic sites. With the addition of TPP, the phosphate sites interact with the amino sites still available.

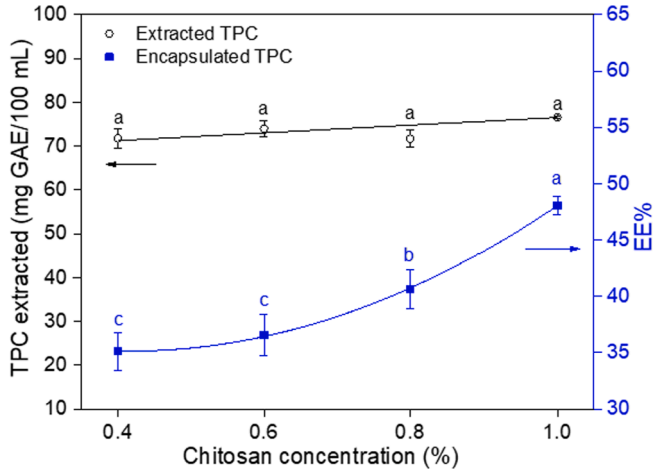

Fig. 1. Effect of chitosan concentration (0.4, 0.6, 0.8 and 1.0 %) on the TPC extraction (mg GAE/100 mL Ch-TPC extract) from acerola by-product and on the encapsulation efficiency (EE%). Dots followed by the same letter indicate no significantly different at $p < 0.05$.

The chitosan concentration was also directly related to the particle size: the higher the polymer concentration, the larger the particle size (Fig. A.2). Although particles produced using 1.0 % of chitosan have the highest EE%, they were significantly thicker than those produced with 0.8 %. Thus, considering the greater possibility of applications with submicro/nanometer scale structures, the particles prepared with 0.8 % chitosan were considered for the further physicochemical characterizations.

3.3. Physicochemical characterization

3.3.1. Phytochemical composition

The phenolics encapsulated in nanoparticles with 0.8 % chitosan are shown in Table 2. All phenolics identified have been previously identified in non-pomace and bagasse of acerola (Poletto et al., 2021).

Through the identification the phenolics it was assumed that there is a high density of negative charge in encapsulated compounds (predominance of groups –OH and -C═O), confirming the hypothesis of interaction with chitosan. In addition, all compounds identified already have some beneficial activity reported in the literature.

5-*p*-Coumaroylquinic acid was identified in methanolic extracts of *Tetrastigma hemsleyanum* leaf, which showed prominent antioxidant activity by ABTS and FRAP assays and antiproliferative activity (Sun et al., 2013). Recently, 2-hydroxycinnamic acid has proved to be an effective antimicrobial in the inhibition of antibiotic-resistant and antibiotic-susceptible *Staphylococcus aureus* vines (Keman & Soyer, 2019), while 4-hydroxycinnamic acid showed anti-inflammatory activity in an *in vivo* model of ovalbumin-induced allergic asthma (Ko et al., 2020). Acerola extracts containing quercetin and kaempferol glucosides have shown a protective effect against oxidative damage by decreasing apoptosis, intracellular reactive oxygen species concentrations and lipid and protein damage, while improving the activity of antioxidant enzymes and mitochondrial functionality in an *in vitro* model using human dermal fibroblast (Alvarez-Suarez et al., 2017). Moreover, those glycosylated flavonols are also recognized by their antifungal properties (Sudheeran et al., 2020).

3.3.2. Morphology

The nanoparticle dimensions obtained by DLS show a trimodal size distribution for Np and Np-TPC (Fig. 2(a)). The Np have a narrower size distribution in which 92 % of the nanoparticles are concentrated around 660 nm. In turn, the encapsulated samples, although with a similar profile, result in larger dimensions with the main peak at 920 nm corresponding to 85 % of the particles' distribution. Similar intensity peaks, centered at 5450 nm, indicate the formation of agglomerates for both samples, in a proportion of about 2.7 %. Both a shift to larger average sizes and the broadening of the distribution are indicative of encapsulation.

The microscopic observation of Np and Np-TPC samples, as displayed in Fig. 2(b), are in agreement with the particle sizes obtained by DLS. The Np has spherical shape, which is characteristic of chitosan nanoparticles (Silva et al., 2021) with dimensions below 100 nm. The Np-TPC samples have a spherical to rod-shaped aspect with individual particles also below 100 nm. The encapsulated nanoparticles, however, present a tendency toward agglomeration as zoomed in Fig. 2(b). The tendency of agglomeration of nanoparticles loaded with active compounds from acerola by-products was also verified in the morphological analysis performed by Silva et al. (2021).

The ease of agglomeration of the encapsulated particles may be due to the low zeta potential measured in these structures (25.6 ± 2.3 mV) compared to the Np (34.8 ± 0.5 mV). The low zeta potential value for the particles with trapped TPC is a result from charge interactions as will be discussed below.

Table 2
Tentative identification by LC/ESI-TOF MS of phytochemicals in the Ch-TPC, with 0.8% chitosan.

Putative compound name	RT (min)	Molecular formula	Error (ppm)	$[M-H]^-$ (*m/z*)	MS fragments (*m/z*)
2-Hydroxycinnamic acid	16.6	$C_9H_8O_3$	8.9	163.0410	119.0509 (100.0), 120.0550 (13.8)
4-Hydroxycinnamic acid	17.2	$C_9H_8O_3$	8.9	163.0410	119.0508 (100.0), 120.0531 (12.7)
Quercetin 3-rhamnoside	22.6	$C_{21}H_{20}O_{11}$	4.1	447.0946	300.0280 (53.2), 301.0375 (100.0), 447.0943 (59.5)
5-*p*-Coumaroylquinic acid	25.8	$C_{16}H_{18}O_8$	5.7	337.0943	161.0480 (100.0), 143.0361 (97.5), 193.0509 (72.5)
Kaempferol-3-rhamnoside	25.7	$C_{21}H_{20}O_{10}$	3.4	431.0993	431.1051 (100.0), 285.0400 (96.7)

RT: retention time.

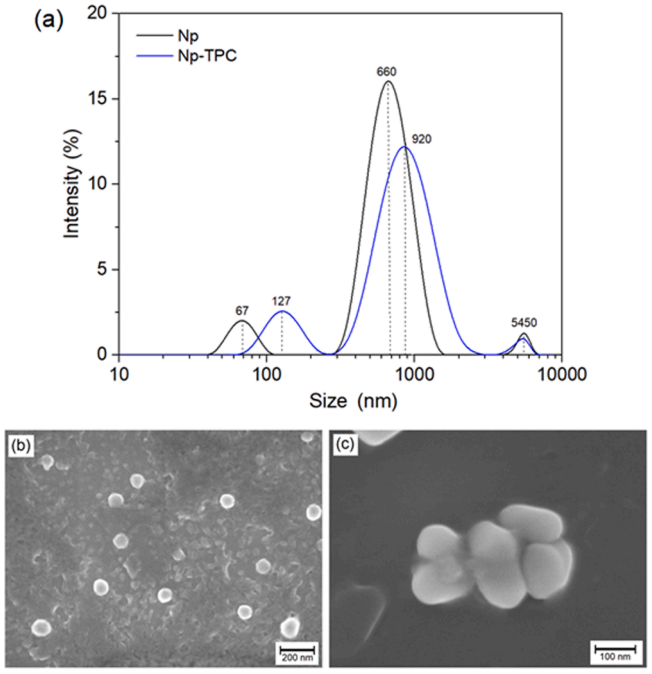

Fig. 2. (a) Particle size distribution of Np and encapsulated Np-TPC, produced with 0.8% chitosan. Correspondent SEM-FEG images of (b) Np and (c) typical formation of particle clusters in the Np-TPC samples.

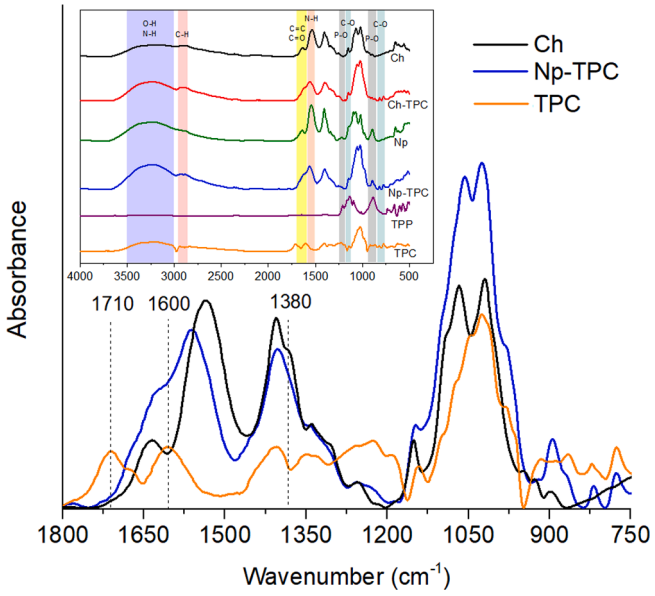

Fig. 3. ATR-FTIR spectra of Ch, TPP solution, Np, Ch-TPC, Np-TPC and neat TPC extract, in the inserted box. The main picture corresponds to the spectral region with the most differences among samples. For all samples the chitosan concentration was 0.8%.

3.3.3. Attenuated total reflection fourier transform infrared spectroscopy (ATR-FTIR)

Fig. 3 shows the resultant spectra of Ch, Ch-TPC, Np, Np-TPC, TPP and TPC (in the inserted box). The intervals of main vibrational groups are highlighted.

The FTIR spectrum of chitosan (Ch) is largely interpreted in literature to present a typical polysaccharide absorbance profile with bands in the region of 3500 to 3000 cm^{-1} corresponding to symmetric stretching vibrations of O—H hydroxyl groups from the H-bonded. The absorbance peak at 2870 cm^{-1} indicates the presence of chain scission of C—H. The vibrational bands are present in all analyzed samples with the exception of TPP.

The band at 1640 cm^{-1} was attributed to the vibration of C═O carbonyl in the amide group (amide I and amide II). The band at 1530 cm^{-1} is characteristic of the N—H bonds of the primary amine, which underwent deprotonation (NH_3^+) after dissolution in acetic acid. Vibrational bands below 1150 cm^{-1} are related to vibrations of stretching O—H, C—H in β-1–4 glycosidic ring, and CH_3 in amide groups, which are characteristic of saccharide structure (Martins, Oliveira, Pereira, Rubira & Muniz, 2012; Antoniou et al., 2015).

A TPP band at around 1100 cm^{-1} is assigned in relation to the symmetric and asymmetric stretching vibrations in the PO_3 group, and a more defined peak at 887 cm^{-1} corresponds to the asymmetric stretching of P—O—P bridge, confirming the presence of phosphate groups. The crosslinking with TPP also changes the vibrations of the C—H and O—H groups from the glycosidic bonds, around 1080 cm^{-1}, as observed when compared to unreacted Ch. Furthermore, peaks in the region of 1650 cm^{-1} became larger than those observed in Ch spectrum due to electrostatic interaction between the TPP phosphate counter ions and the amino groups in Ch (Cho et al., 2014).

Concerning the main interactions of Ch, neat TPC and TPC nanoparticle entrapped (Np-TPC), a zoomed picture of the main interacting region is depicted in Fig. 3. Although the dominant peaks of chitosan were preserved, when interacting with TPP and TPC some changes can be observed concerning band shapes and intensities.

The spectrum of neat TPC is characterized by the presence of numerous bands that are not well defined, mainly in the 1800–750 cm^{-1} range. The most intense band at 1030 cm^{-1} corresponds to the benzene ring vibration, and the broad band centered around 1230 cm^{-1} is assigned as C—O stretching (Martí et al., 2014). The peaks centered at 1710 and 1600 cm^{-1} is attributed to the deformation vibrations of OH groups overlapping the vibrations related to C═C alkene moieties (Zarina, Ruzaidi, Sam & Al Bakri, 2019) and C═O carbonyl groups (Kozłowicz et al., 2020) in the polyphenol compound.

When incorporated inside the chitosan crosslinked nanoparticles (Np-TPC), the peak related to N—H bending from amine and amide II in chitosan has the intensity reduced and shifted to longer wavelengths. The resultant vibration has a broad band range, overlapping the original chitosan amide stretching (at 1640 cm^{-1}), resulting in a shoulder in the load system. Additionally, a peak at 1380 cm^{-1}, corresponding to CH_3 symmetrical deformation in the chitosan backbone, vanishes in encapsulated nanoparticles. According to Kosaraju, D'ath, L. & Lawrence (2006), all of these events are related to potential H-bond or ionic interactions between hydroxyl and carboxyl bonds of the polyphenols and

the amine functionality of the chitosan molecule.

In summary, the FTIR analyses confirm the incorporation of TPC inside chitosan nanoparticles, although it does not clearly reveal whether there is any competition between groups of TPP and the polyphenols in the interaction with chitosan.

3.3.4. Accelerated stability

Fig. 4(a) and (b) show the evolution of the transmission profile during centrifugation of the suspensions of Np and Np-TPC, respectively.

A polydisperse sedimentation is observed when the transmission is practically constant along the position of the sample in the cell, as seen for both suspensions. In Fig. 4(a) and (b), the drop in transmission values at 129 nm occurs as a result from the phase separation in the sample, indicating sedimentation of the particles. The polydisperse behavior indicates that particles of different sizes are present in suspension. This was confirmed by the Polydispersity Index (PI) of suspensions obtained by zeta potential analyser, whose value > 0.2 (0.40 for Np and 0.48 for Np-TPC) indicates the heterogeneity of the system (Sobisch & Lerche, 2008; Zielinska et al. 2019). The heterogeneous profile of the particles is reflected in high levels of instability. According to Zielinska et al. (2019), this is expected for systems with larger particle sizes and high PI values. For both systems, the instability index was 0.81. The similar profiles of Np and Np-TPC indicated that the presence of the actives does not change the stability of the system under accelerated conditions.

3.3.5. Release profile

The release profile is related to the ability of the particles to deliver the entrapped compound in a controlled way to the medium. Fig. 5 shows the proportional amount of TPC released from the encapsulated system during 10 h, tested in acidic and subsequent neutral media.

Both sets of data can be adjusted to a linear model ($y = a + sx$), for simple mathematical consideration. The correlation parameter ($R^2 > 0.9$) confirmed the feasibility of this fitting. The "s" parameter (slope) is associated with the curve inclination and is the measure of the rate in which the dependent variable (TPC delivery) changes in function of time in the tested medium. Given the respective values inserted in Fig. 5, the slope at pH 3.0 is approximately 9 times higher than that obtained in neutral medium (pH 7.0).

Numerically, about 35 % of the encapsulated TPC were released within the first hour of the experiment. From this point on, the release rate according to the linear fitting is around 20.72 % at pH 3.0. Since chitosan is soluble in acidic pH, it is assumed that the particles are broken down by facilitating the release of TPC. By changing to pH 7.0, the release rate, evidently, becomes slower and drops to 2.30 %/h, until all compounds were completely free in suspension. As expected, the results confirm the pH dependency of the active release from chitosan encapsulation.

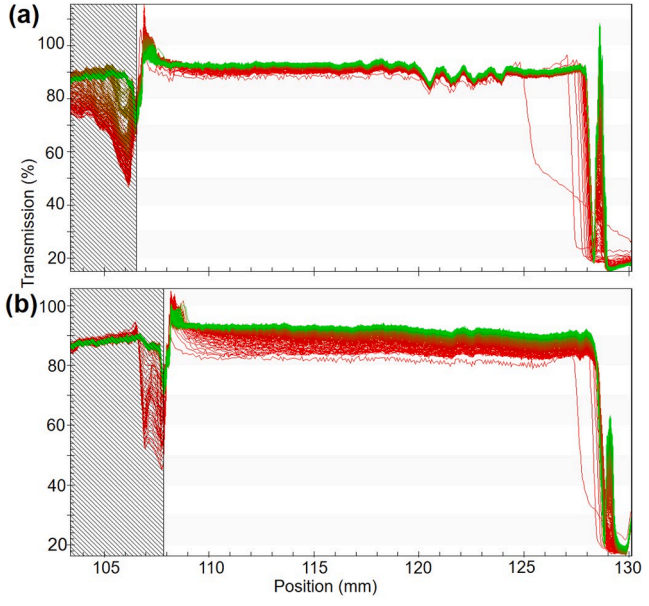

Fig. 4. Stability profile of the suspension of (a) Np and (b) Np-TPC, with 0.8 % chitosan, by LUMiSizier at 25 °C.

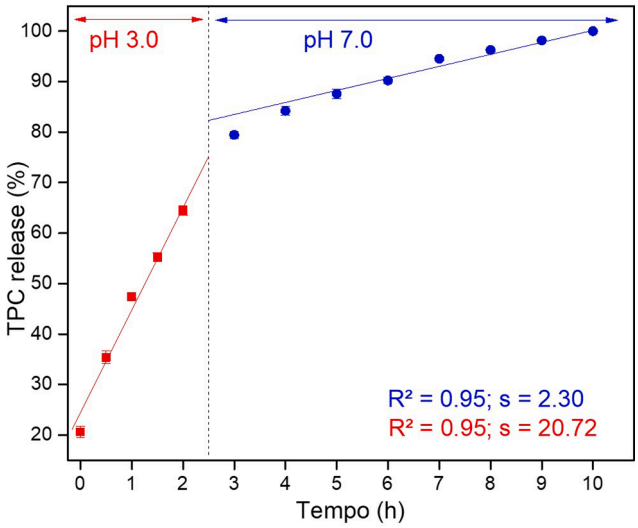

Fig. 5. TPC release profile, considering the amount released from the total encapsulated as a function of time (h), at pH 3.0 (between 0 and 2 h) and pH 7.0 (between 2 and 10 h) at 37 °C. Data adjusted by linear regression.

4. Conclusion

The chitosan concentrations used in this study (0.4 – 1.0 %) did not affect the quantity of phenolic compounds extracted from acerola by-products, indicating that the acetic acid medium was the responsible for the active compound extraction. However, the higher the chitosan concentration, the greater the encapsulation efficiency (up to 48.1 ± 0.8 %). These results can be explained by the higher amount of available NH_3^+ sites to interact with the phenolic compounds.

In general, the choice of Ch concentration in extraction/encapsulation depends on the final application. Although the suspension with higher chitosan concentration had the greater EE%, the particles formed were larger, which may be an indication of greater instability and possible agglomeration. Besides, the 0.8 % chitosan presented acceptable values of EE% and particles with diameters in the nanoscale. Moreover, these particles showed good stability when subjected to accelerated conditions. The stability as a function of different pH demonstrated the dependence of the active release in these cases, with most of the phenolic compounds being released at acidic pH (3.0) probably due to the better solubility of the chitosan in this condition.

CRediT authorship contribution statement

Natalia Cristina da Silva: Conceptualization, Data curation, Formal analysis, Investigation, Methodology, Validation, Visualization, Writing – original draft, Writing – review & editing. **Odílio Benedito Garrido Assis:** Conceptualization, Data curation, Formal analysis, Resources, Supervision, Validation, Visualization, Writing – original draft, Writing – review & editing. **Alan Giovanini de Oliveira Sartori:** Formal analysis, Investigation, Methodology, Validation, Visualization, Writing – original draft, Writing – review & editing. **Severino Matias de Alencar:** Formal analysis, Investigation, Methodology, Validation, Visualization, Writing – original draft, Writing – review & editing. **Milena Martelli-Tosi:** Conceptualization, Data curation, Formal analysis, Funding

acquisition, Investigation, Project administration, Resources, Supervision, Validation, Visualization, Writing – original draft, Writing – review & editing.

Declaration of Competing Interest

The authors declare that they have no known competing financial interests or personal relationships that could have appeared to influence the work reported in this paper.

Data availability

Data will be made available on request.

Acknowledgments

The authors gratefully acknowledge the MCTI SisNano, Rede Agronano (Embrapa Research Network), University of São Paulo, São Paulo Research Foundation – FAPESP (grant numbers 2016/18788-1 and 2019/23171-1) and the Coordination for the Improvement of Higher Education Personnel (CAPES) for the doctoral fellowship granted to Silva, N. C (Finance Code 001).

Appendix A. Supplementary data

Supplementary data to this article can be found online at https://doi.org/10.1016/j.foodres.2022.111855.

References

Abreu, B. B., Moreira, L. R. L. F., Cavalcante, R. B. M., Campos, C. M. F., & Gonçalves, M. F. B. (2020). Desenvolvimento de um "nugget" à base do resíduo da acerola (Malpighia emarginata D.C) e feijão-caupi (Vigna unguiculata L.). *Brazilian Journal of Development, 6*, 9446–9453. https://doi.org/10.34117/bjdv6n2-307.

Akcicek, A., Bozkurt, F., Akgül, C., & Karasu, S. (2021). Encapsulation of Olive Pomace Extract in Rocket Seed Gum and Chia Seed Gum Nanoparticles: Characterization, Antioxidant Activity and Oxidative Stability. *Foods, 10,* Article 1735. https://doi.org/10.3390/foods10081735.

Alvarez-Suarez, J. M., Giampieri, F., Gasparrini, M., Mazzoni, L., Santos-Buelga, C., González-Paramás, A. M., et al. (2017). The protective effect of acerola (Malpighia emarginata) against oxidative damage in human dermal fibroblasts through the improvement of antioxidant enzyme activity and mitochondrial functionality. *Food & Function, 8*, 3250–3258. https://doi.org/10.1039/c7fo00859g

Antoniou, J., Liu, F., Majeed, H., Qi, J., Yokoyama, W., & Zhong, F. (2015). Physicochemical and morphological properties of size-controlled chitosan-tripolyphosphate nanoparticles. *Colloids and Surfaces A: Physicochemical and Engineering Aspects, 465*, 137–146. https://doi.org/10.1016/j.colsurfa.2014.10.040

AOAC. official methods of analysis of AOAC International. Association of Official Analytical Chemists, ed. 16, Washington, 1997.

Baierle, M., Bairros, A., Moreira, A. P., Bulcão, R., Roehrs, M., Freitas, F., et al. (2012). Quantificação sérica de vitamina C por CLAE-UV e estudo de estabilidade. *Química Nova, 35*, 403–407. https://doi.org/10.1590/S0100-40422012000200030

Bozic, M., Gorgieva, S., & Kokol, V. (2012). Laccase-mediated functionalization of chitosan by caffeic and gallic acids for modulating antioxidant and antimicrobial properties. *Carbohydrate Polymers, 87*, 2388–2398. https://doi.org/10.1016/j.carbpol.2011.11.006

Britto, D., Moura, M. R., Aouada, F. A., Pinola, F. G., Lundstedt, L. M., Assis, O. B. G., et al. (2014). Entrapment characteristics of hydrosoluble vitamins loaded into chitosan and N, N, N-trimethyl chitosan nanoparticles. *Macromolecular Research, 22*, 1261–1267. https://doi.org/10.1007/s13233-014-2176-9

Caddeo, C. (2016). Effect of quercetin and resveratrol co-incorporated in liposomes against inflammatory/oxidative response associated with skin cancer. *International Journal of Pharmaceutics, 513*, 153–163. https://doi.org/10.1016/j.ijpharm.2016.09.014

Cho, A. R., Chun, Y. G., Kim, B. K., & Park, D. J. (2014). Preparation of chitosan–TPP microspheres as resveratrol carriers. *Journal of Food Science, 79*, E568–E576. https://doi.org/10.1111/1750-3841.12395

Esposto, B. S., Jauregi, P., Tapia-Blácido, D. R., & Martelli-Tosi, M. (2021). Liposomes vs. chitosomes: Encapsulating food bioactives. *Trends in Food Science and Technology, 108*, 40–48. https://doi.org/10.1016/j.tifs.2020.12.003

Esposto, B. S., Pinho, S. G. B., Thomazini, M., Ramos, A. P., Tapia-Blácido, D. R., & Martelli-Tosi, M. (2022). TPP-chitosomes as potential encapsulation system to protect carotenoid-rich extract obtained from carrot by-product: A comparison with liposomes and chitosomes. *Food Chemistry, 397*, Article 133857. https://doi.org/10.1016/J.FOODCHEM.2022.133857

Funari, C. S., & Ferro, V. (2006). Análise de Própolis. *Ciência e Tecnologia de Alimentos, 26,* 171–178. . Accessed July 12, 2022.

Gualberto, N. C., Oliveira, C. S., Nogueira, J. P., Jesus, J. M., Araujo, H. C. S., Rajan, M., Neta, M. T. S. L., & Narain, N. Bioactive compounds and antioxidant activities in the agro-industrial residues of acerola (Malpighia emarginata L.), guava (Psidium guajava L.), genipap (Genipa americana L.) and umbu (Spondias tuberosa L.) fruits assisted by ultrasonic or shaker extraction. *Food Research International, 147,* Article 110538. https://doi.org/10.1016/j.foodres.2021.110538.

Javadian, S. R., Shahosseini, S. R., & Ariaii, P. (2017). The effects of liposomal encapsulated thyme extract on the quality of fish mince and Escherichia coli O157: H7 inhibition during refrigerated storage. *Journal of Aquatic Food Product Technology, 26*, 115–123. https://doi.org/10.1080/10498850.2015.1101629

Keman, D., & Soyer, F. (2019). Antibiotic-resistant staphylococcus aureus does not develop resistance to vanillic acid and 2-hydroxycinnamic acid after continuous exposure in vitro. *ACS Omega, 4*, 15393–15400. https://doi.org/10.1021/acsomega.9b01336

Ko, J. W., Kwon, H. J., Seo, C. S., Choi, S. J., Shin, N. R., Kim, S. H., et al. (2020). 4-Hydroxycinnamic acid suppresses airway inflammation and mucus hypersecretion in allergic asthma induced by ovalbumin challenge. *Phytotherapy Research, 34*, 624–633. https://doi.org/10.1002/ptr.6553

Kosaraju, S. L., D'ath, L., & Lawrence, A. (2006). Preparation and characterisation of chitosan microspheres for antioxidant delivery. *Carbohydrate Polymers, 64*, 163–167. https://doi.org/10.1016/j.carbpol.2005.11.027

Kozłowicz, K., Różyło, R., Gładyszewska, B., Matwijczuk, A., Gładyszewski, G., Chocyk, C., Samborska, K., Piekut, J., & Smolewska, M. (2020). Identification of sugars and phenolic compounds in honey powders with the use of GC–MS, FTIR spectroscopy, and X-ray diffraction. *Scientific Reports, 10,* Article 16269. https://doi.org/10.1038/s41598-020-73306-7.

Lee, J., Durst, R. W., & Wrolstad, R. E. (2005). Determination of total monomeric anthocyanin pigment content of fruit juices, beverages, natural colorants, and wines by the pH differential method: Collaborative study. *Journal of AOAC International, 88*, 1269–1278. https://doi.org/10.1093/jaoac/88.5.1269

Liang, J., Yan, H., Puligundla, P., Gao, X., Zhou, Y., & Wan, X. (2017). Applications of chitosan nanoparticles to enhance absorption and bioavailability of tea polyphenols: A review. *Food Hydrocolloids, 69*, 286–292. https://doi.org/10.1016/j.foodhyd.2017.01.041

Lima, M. C., Magnani, M., Lima, M. S., Sousa, C. P., Dubreuil, J. D., & Souza, E. L. (2021). Phenolic-rich extracts from acerola, cashew apple and mango by-products cause diverse inhibitory effects and cell damages on enterotoxigenic Escherichia coli. *Letters in Applied Microbiology, 74*(2), 1–13. https://doi.org/10.1111/lam.13586

Liu, H., & Gao, G. (2008). Preparation and properties of ionically cross-linked chitosan nanoparticles. *Polymer Advanced Technologies, 20*, 613–619. https://doi.org/10.1002/pat.1306

Martí, M., Martínez, V., Carreras, N., Alonso, C., Lis, M. J., Parra, J. L., et al. (2014). Textiles with gallic acid microspheres: In vitro release characteristics. *Journal of Microencapsulation, 31*, 535–541. https://doi.org/10.3109/02652048.2014.885605

Maleki, G., Woltering, E. J., & Mozafari, M. R. (2022). Applications of chitosan-based carrier as an encapsulating agent in food industry. *Trends in Food Science & Technology, 120*, 88–99. https://doi.org/10.1016/J.TIFS.2022.01.001

Martins, A. F., Oliveira, D. M., Pereira, A. G. B., Rubira, A. F., & Muniz, E. C. (2012). Chitosan/TPP microparticles obtained by microemulsion method applied in controlled release of heparin. *International Journal of Biological Macromolecules, 51*, 1127–1133. https://doi.org/10.1016/j.ijbiomac.2012.08.032

Mendes, A. M. S., et al. (2012). *Coleção Plantar – A Cultura da Acerola* ((3th ed).). Embrapa Produção de Informação.

Monteiro, S. A., Barbosa, M. M., Silva, F. F. M., Bezerra, R. F., & Maia, K. S. (2020). Preparation, phytochemical and bromatological evaluation of flour obtained from the acerola (Malpighia punicifolia) agroindustrial residue with potential use as fiber source. *Food Science and Technology, 134*, 1–7. https://doi.org/10.1016/j.lwt.2020.110142

Poletto, P., Álvarez-Rivera, G., López, G., Borges, O. M. A., Mendiola, J. A., Ibañez, E., et al. (2021). Recovery of ascorbic acid, phenolic compounds and carotenoids from acerola by-products: An opportunity for their valorization. *Food Science and Technology, 146*, Article 111654. https://doi.org/10.1016/j.lwt.2021.111654

Pulicharla, R., Marques, C., Das, R. K., Rouissi, T., & Brar, S. K. (2016). Encapsulation and release studies of strawberry polyphenols inbiodegradable chitosan nanoformulation. *International Journal of Biological Macromolecules, 88*, 171–178. https://doi.org/10.1016/j.ijbiomac.2016.03.036

Pulido, R., Bravo, L., & Saura-Calixto, F. (2000). Antioxidant activity of dietary as determined by a modified ferric reducing/antioxidant power assay. *Journal Agriculture and Food Chemistry, 48*, 3396–3402. https://doi.org/10.1021/jf9913458

Re, R., Pellegrini, N., Proteggente, A., Pannala, A., Yang, M., & Rice-Evans, C. (1999). Antioxidant activity applying an improved ABTS radical cation decolorization assay. *Free Radical Biology & Medicine, 26*, 1231–1237. https://doi.org/10.1016/s0891-5849(98)00315-3

Rezende, Y. R. R. S., Nogueira, J. P., & Narain, N. (2017). Comparison and optimization of conventional and ultrasound assisted extraction for bioactive compounds and antioxidant activity from agro-industrial acerola (Malpighia emarginata DC) residue. *Food Science and Technology, 85*, 158–169. https://doi.org/10.1016/j.lwt.2017.07.020

Rodrigues, E., Mariutti, L. R. B., & Mercadante, A. Z. (2013). Carotenoids and Phenolic Compounds from Solanum sessiliflorum, an Unexploited Amazonian Fruit, and Their Scavenging Capacities against Reactive Oxygen and Nitrogen Species. *Journal of Agricultural and Food Chemistry, 61*, 3022–3029. https://doi.org/10.1021/jf3054214

Silva, N. C., Barros-Alexandrino, T. T., Assis, O. B. G., & Martelli-Tosi, M. (2021). Extraction of phenolic compounds from acerola by-products using chitosan solution, encapsulation and application in extending the shelf-life of guava. *Food Chemistry, 354*, Article 129553. https://doi.org/10.1016/j.foodchem.2021.129553

Silva, N. C., & Martelli-Tosi, M. (2021). Extraction of phenolic compounds from acerola pulp residues: encapsulation in chitosan micro/nanoparticles. Brazilian Patent Application No. BR 10 2021 011708 7. Instituto Nacional da Propriedade Industrial (INPI), Brazil.

Skendi, A., Irakli, M., Chatzopoulou, P., Bouloumpasi, E., & Biliaderis, C. G. (2022). Phenolic extracts from solid wastes of the aromatic plant essential oil industry: Potential uses in food applications. *Food Chemistry Advances, 1*, Article 100065. https://doi.org/10.1016/J.FOCHA.2022.100065

Soares, J. C., et al. (2019). Comprehensive characterization of bioactive phenols from new Brazilian superfruits by LC-ESI-QTOF-MS, and their ROS and RNS scavenging effects and anti-inflammatory activity. *Food Chemistry, 281*, 178–188. https://doi.org/10.1016/j.foodchem.2018.12.106

Sobisch, T., & Lerche, D. (2008). Thickener performance traced by multisample analytical centrifugation. *Colloids and Surfaces A: Physicochem and Engineering Aspects, 331*, 114–118. https://doi.org/10.1016/j.colsurfa.2008.05.040

Shahosseini, S. R., Javadian, S. R., & Safari, R. (2022). Effects of Molecular Weights-Assisted Enzymatic Hydrolysis on Antioxidant and Anticancer Activities of Liza abu Muscle Protein Hydrolysates. *International Journal of Peptide Research and Therapeutics, 28*, 1–11. https://doi.org/10.1007/s10989-022-10371-8

Sudheeran, P. K., Ovadia, R., Galsarker, O., Maoz, I., Sela, N., Maurer, D., et al. (2020). Glycosylated flavonoids: Fruit's concealed antifungal arsenal. *New Phytologist, 225*, 1788–1798. https://doi.org/10.1111/nph.16251

Sun, Y., Li, H., Hu, J., Li, J., Fan, Y. W., Liu, X. R., et al. (2013). Qualitative and quantitative analysis of phenolics in Tetrastigma hemsleyanum and their antioxidant and antiproliferative activities. *Journal of Agricultural and Food Chemistry, 61*, 10507–10515. https://doi.org/10.1021/jf4037547

Swain, T., & Hillis, W. E. (1959). The phenolic constituents of Prunus domestica I.—The quantitative analysis of phenolic constituents. *Journal of the Science of Food and Agriculture, 10*, 63–68. https://doi.org/10.1002/jsfa.2740100110

Zarina, Z., Ruzaidi, C. M., Sam, S. T., & Al Bakri, A. M. M. (2016). Investigation on antioxidants compounds composition contains in Leucaena Leucocephala (Petai Belalang). *IOP Conf. Series: Materials Science and Engineering, 551,* Article 012016. https://doi.org/10.1088/1757-899X/551/1/012016.

Zielinska, A., Martins-Gomes, C., Ferreira, N. R., Silva, A. M., Nowak, I., & Souto, E. (2019). Anti-inflammatory and anti-cancer activity of citral: Optimization of citralloaded solid lipid nanoparticles (SLN) using experimental factorial design and LUMiSizer. *International Journal of Pharmaceutics, 553*, 428–440. https://doi.org/10.1016/j.ijpharm.2018.10.065